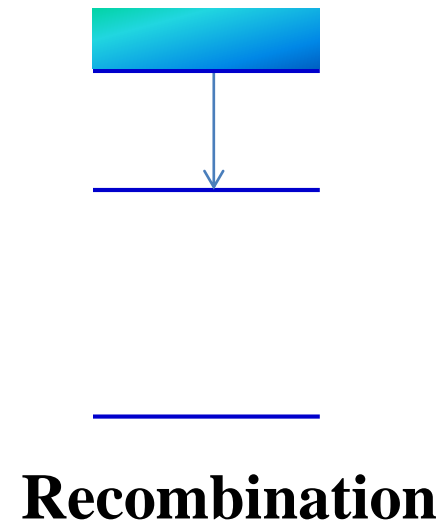
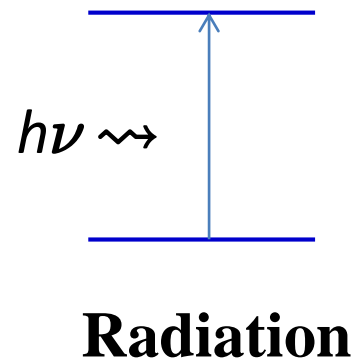
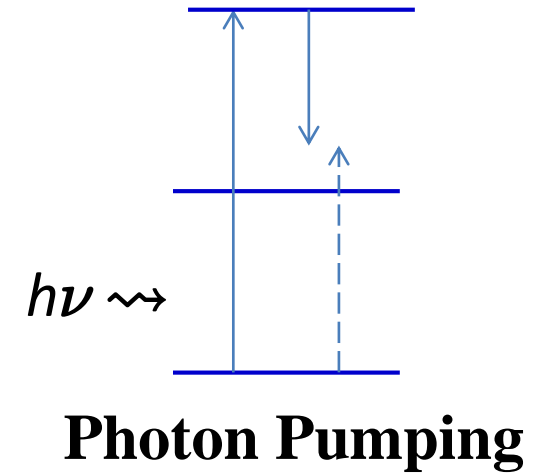
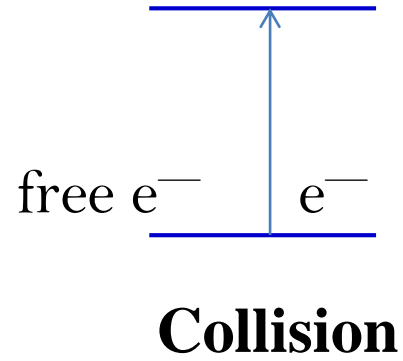
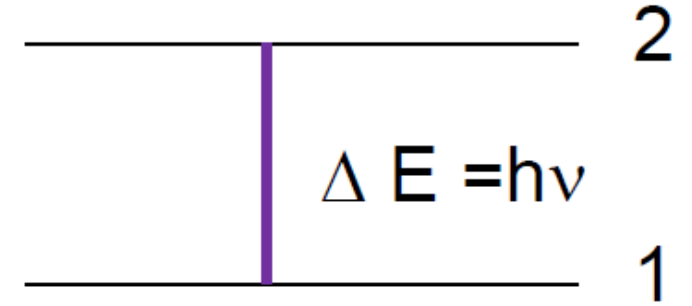


Excitations



Emission and Absorption

Two ways to decay down from an excited state

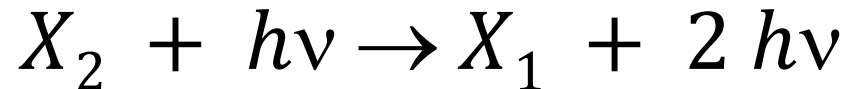


- **Spontaneous emission**



occurrence rate \leftrightarrow atomic properties

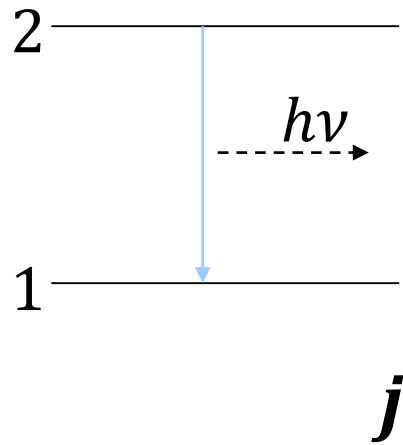
- **Stimulated emission**



occurrence rate \leftrightarrow density of incoming photons of the same ν , polarization, and direction of propagation

Einstein Coefficients

Spontaneous emission

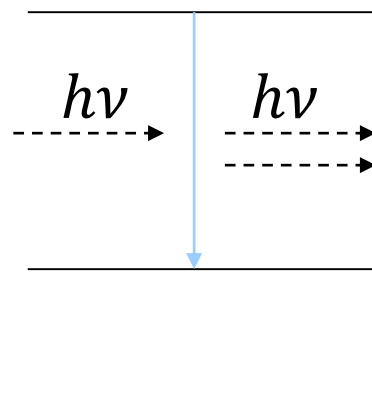


$$A_{21}$$

$$[s^{-1}]$$

A_{21} --- probability

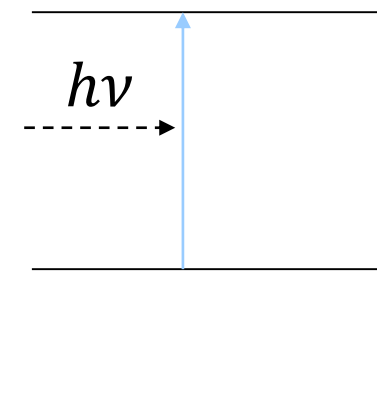
Stimulated (induced) emission (Stimulated) absorption



$$B_{21}$$

$$[cm^3 \text{ erg } s^{-1} \text{ Hz}^{-1}]$$

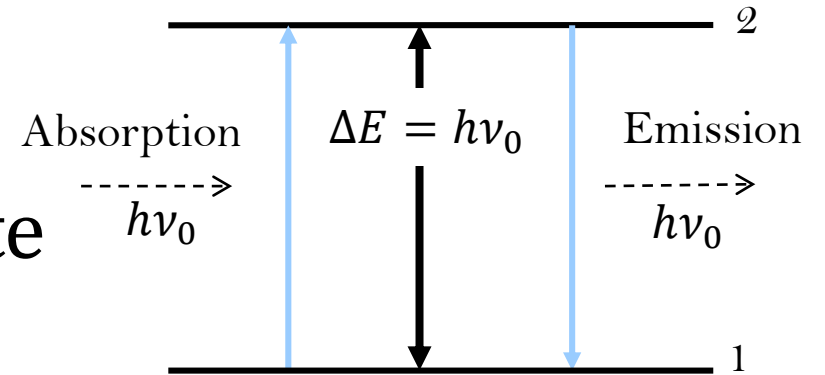
$B u_\nu$ --- probability



$$B_{12}$$

Transition Probability

Considering a 2-level system, we calculate the emission arising from the transition.

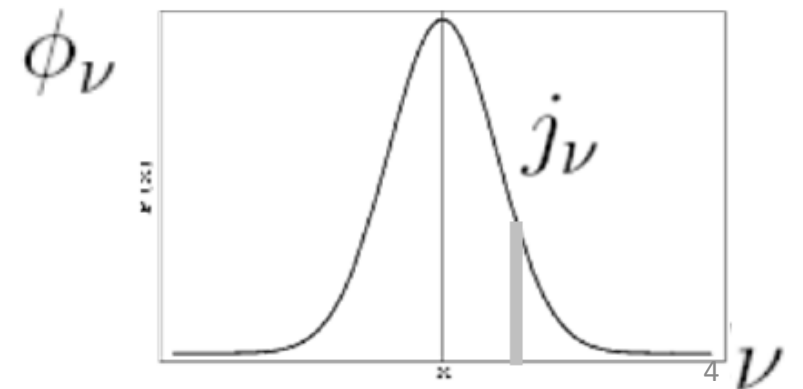


$$j_\nu \text{ [erg s}^{-1} \text{ cm}^{-3} \text{ ster}^{-1} \text{ Hz}^{-1}\text{]}$$

$$j = \int j_\nu d\nu \text{ [erg s}^{-1} \text{ cm}^{-3} \text{ ster}^{-1}\text{]} \text{ volume emissivity}$$

For a line emission, assuming $j_\nu \leftrightarrow \theta, \varphi$, j_ν is governed by a distribution function $\phi(\nu)$ (**line profile**),

$$\int_0^\infty \Phi_\nu d\nu = 1$$



Once an atom is excited, there is a finite probability within dt , $A(2,1) dt$ to jump spontaneously from level 2 to level 1 (deexcitation), emitting a photon. The total number of downward transitions $2 \rightarrow 1$ is $n_2 A(2,1)$, where n_2 is the number of atoms (population) in level 2 per unit volume.

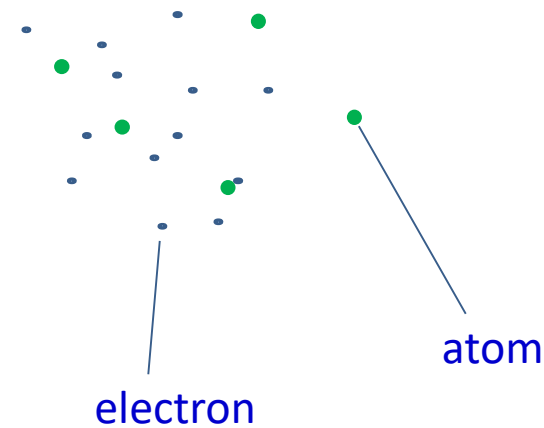
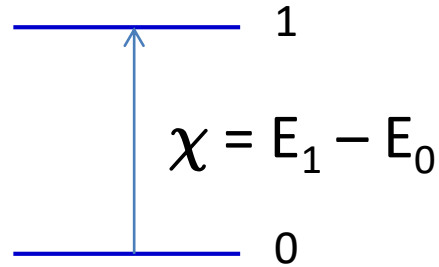
**$A_{21} [s^{-1}]$: Einstein A coefficient for spontaneous transition
= probability per unit time.**

$1/A_{21} [s]$: lifetime staying at level 2 (remaining excited)

$$j_\nu = \frac{h\nu_0}{4\pi} n_2 A_{21} \phi(\nu)$$

Principle of detailed balancing

Consider a 2-level system, excitation occurs if the incoming free electrons have kinetic energy $\frac{1}{2} m v^2 > \chi$



Define the **excitation rate coefficient** γ_{01} , so that

of excitation $\text{s}^{-1} \text{cm}^{-3}$ ($= n_e n_0 v \sigma$) $\equiv n_e n_0 \gamma_{01}$,
where both n_e and n_0 have units of $[\text{cm}^{-3}]$

$$\gamma_{01} \equiv \langle \sigma v \rangle = \int_{\chi=\frac{1}{2}mv^2}^{\infty} \sigma_{01}(v) v f(\vec{v}) d^3 \vec{v}$$

Here σ_{01} is the excitation cross section, and $f(\vec{v})$ is the Maxwellian distribution function,

$$f(\vec{v}) dv = 4\pi \left(\frac{m}{2\pi kT} \right)^{3/2} v^2 e^{-\frac{mv^2}{2kT}} dv$$

So

$$\gamma_{01} = \frac{4}{\sqrt{\pi}} \left(\frac{1}{2kT} \right)^{1/2} \int_{\chi=\frac{1}{2}mv^2}^{\infty} v^3 \sigma_{01}(v) e^{-\frac{mv^2}{2kT}} dv \quad \dots (A)$$

This is upward $0 \rightarrow 1$ transition.

For downward $1 \rightarrow 0$ transition,
the spontaneous emission rate = $n_1 A_{10}$,
and the deexcitation rate by collisions = $n_1 n_e \gamma_{10}$,

$$\text{where } \gamma_{10} = \int_0^\infty v \sigma_{10}(v) f(\vec{v}) d^3 \vec{v} = \gamma_{10}(T)$$

In steady state, [upwards rate]=[downwards rate],
i.e., **detailed balancing**,

$$n_0 n_e \gamma_{01}(T) = n_1 [A_{10} + n_e \gamma_{10}(T)], \text{ so}$$

$$\frac{n_1}{n_0} = \frac{n_e \gamma_{01}}{A_{10} + n_e \gamma_{10}} = \frac{\gamma_{01}}{\gamma_{10}} \frac{1}{1 + \frac{A_{10}}{n_e \gamma_{10}}} \quad \dots \text{(B)}$$

$$\frac{n_1}{n_0} = \frac{n_e \gamma_{01}}{A_{10} + n_e \gamma_{10}} = \frac{\gamma_{01}}{\gamma_{10}} \frac{1}{1 + \frac{A_{10}}{n_e \gamma_{10}}}$$

(i) At **high** densities, i.e., $n_e \rightarrow \infty$

(i.e., collisional excitation and deexcitation dominate \rightarrow in TE)

$$\frac{n_1}{n_0} \approx \frac{\gamma_{01}}{\gamma_{10}}$$

but because $\frac{n_1}{n_0} = \frac{g_1}{g_0} e^{-\chi/kT}$

$$\frac{\gamma_{01}}{\gamma_{10}} = \frac{g_1}{g_0} e^{-\chi/kT} \quad \text{for } n_e \gg 1$$

So when collision dominates, c.f. (A)

$$\begin{aligned} n_e n_0 v_0^3 \sigma_{01}(v_0) \exp(-\mu v_0^2 / (2kT)) dv_0 \\ = n_e n_1 v_1^3 \sigma_{10}(v_1) \exp(-\mu v_1^2 / (2kT)) dv_1 \end{aligned}$$

where μ : reduced mass, v_0 and v_1 are speed of colliding particles.

At high densities (*cont.*)

Energy conservation, $(1/2) \mu v_0^2 = (1/2) \mu v_1^2 + \chi$,
so $v_0 dv_0 = v_1 dv_1$. Plugging this back, we get

$$\begin{aligned} n_0 v_0^2 \sigma_{01} \exp\left(-\frac{\mu v_0^2}{2kT}\right) &= n_1 v_1^2 \sigma_{10} \exp\left(-\frac{\mu v_1^2}{2kT}\right) \\ &= n_0 \frac{g_1}{g_0} e^{-\chi/kT} v_1^2 \sigma_{10} \exp\left(-\frac{\mu v_1^2}{2kT}\right) \end{aligned}$$

The exponential parts are eliminated from energy conservation, so

$$g_0 v_0^2 \sigma_{01} = g_1 v_1^2 \sigma_{10}$$

$$\frac{n_1}{n_0} = \frac{n_e \gamma_{01}}{A_{10} + n_e \gamma_{10}} = \frac{\gamma_{01}}{\gamma_{10}} \frac{1}{1 + \frac{A_{10}}{n_e \gamma_{10}}}$$

(i) At **low** densities, i.e., $n_e \rightarrow 0$

$$\frac{n_1}{n_0} \approx \frac{\gamma_{01}}{\gamma_{10}} \frac{n_e \gamma_{10}}{A_{10}} = \frac{n_e \gamma_{01}}{A_{10}} = \frac{\text{[upward by collisions]}}{\text{[downward by radiation only]}}$$

This means every collisional excitation is followed by emission of a photon.

The cooling rate [$\text{erg s}^{-1} \text{ cm}^{-3}$] in this case then, is

$$n_1 A_{10} h\nu_{10} = n_e n_0 \gamma_{01} h\nu_{10}$$

$$n_0 n_e \gamma_{01}(T) = n_1 [A_{10} + n_e \gamma_{10}(T)]$$

The competition for downward transition between the two terms in the bracket \rightarrow the critical density

$$n_{\text{crit}} = \frac{A_{10}}{\gamma_{10}}$$

When $n_e > n_{\text{crit}}$, collisions dominate deexcitation process \rightarrow LTE, populations governed by Boltzmann equation.

Consider the radiative transition $1 \rightarrow 0$, the rate of emission of line photons [$s^{-1} \text{atom}^{-1}$] ... cf. eq. (B)

$$\frac{n_1}{n_0} = \frac{n_e \gamma_{01}}{A_{10} + n_e \gamma_{10}} = \frac{\gamma_{01}}{\gamma_{10}} \frac{1}{1 + \frac{A_{10}}{n_e \gamma_{10}}} \quad \dots \text{(B)}$$

$$\frac{n_1}{n_0} A_{10} = A_{10} \frac{\gamma_{01}}{\gamma_{10}} \frac{1}{1 + \frac{A_{10}}{n_e \gamma_{10}}}$$

(i) At high densities, TE

$$\frac{n_1}{n_0} A_{10} = A_{10} \frac{\gamma_{01}}{\gamma_{10}} = A_{10} \frac{g_1}{g_2} e^{-\chi/kT} \quad \left\langle \times \right\rangle n_e$$

(ii) At low densities,

$$\frac{n_1}{n_0} A_{10} = A_{10} \frac{\gamma_{01}}{\gamma_{10}} \frac{n_e \gamma_{10}}{A_{10}} = n_e \gamma_{01} \quad \left\langle \times \right\rangle T$$

Every collisional excitation \rightarrow emission of a line photon.

Consider a 2-level system, for which the electron collides with an ion in the lower level. cross section, $\sigma_{01} = \sigma_{01}(v)$.

Consider electron v only; ions are neglected.

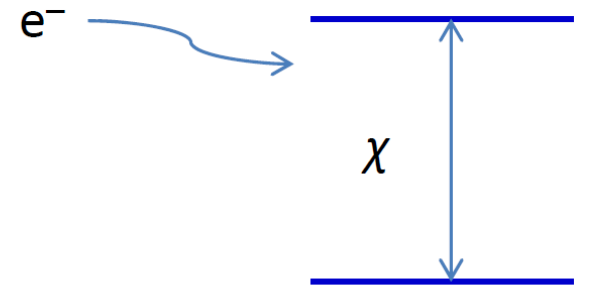
$$\begin{cases} \sigma_{01} = 0, & \text{if } (1/2) m v^2 < \chi \\ \sigma_{01} \propto 1/v^2, & \text{if } (1/2) m v^2 > \chi \end{cases}$$

Usually σ is expressed in terms of **collision strength** $\Omega(0,1)$,

$$\sigma_{01}(v) = \frac{\pi \hbar^2}{m_e^2 v_0^2} \frac{\Omega(0,1)}{g_0} = \frac{4.21 \Omega(0,1)}{v^2 g_0} \text{ [cm}^2\text{]}$$

Recall that $g_0 v_0^2 \sigma_{01} = g_1 v_1^2 \sigma_{10}$

Collisions between electrons and ions in a lower level



The deexcitation rate coefficient is

$$\begin{aligned}\gamma_{10} &= \int_0^{\infty} v \sigma_{10}(v) f(v) dv \\ &= \sqrt{\frac{2\pi}{kT}} \frac{\hbar^2}{m^{3/2}} \frac{\Omega(0,1)}{g_1} = 8.629 \times 10^{-6} \frac{\Omega(0,1)}{g_1 T^{1/2}}\end{aligned}$$

Excitation per volume per time is $n_e n_0 \gamma_{01}$, where

$$\gamma_{01} = (g_1/g_0) \gamma_{10} \exp(-\chi/kT)$$

- Ω must be calculated quantum mechanically;
- tabulation available with specific temperature values;
- typically on the order of unity.

The collisional deexcitation rate is then

$$\begin{aligned} n_e n_1 \gamma_{10} &= n_1 \int_0^\infty n_e v \sigma_{10}(v) f(v) dv \\ &= n_e n_1 \sqrt{\frac{2\pi}{kT} \frac{\hbar^2}{m^{3/2}} \frac{\Omega(1,0)}{g_1}} \\ &= 8.629 \times 10^{-6} \frac{n_e n_1}{g_1 T^{1/2}} \Omega(1,0) \quad [\text{cm}^{-3} \text{s}^{-1}] \end{aligned}$$

For typical nebular $T = 7000$ K, and abundances,

$$\gamma_{10} \approx 10^{-7} \text{ cm}^3 \text{ s}^{-1}$$

Table 8. Wavelengths, λ_{ij} , transition probabilities, A_{ij} , and collision strengths, $\Omega(i,j)$, for the forbidden transitions of the most abundant elements¹

Element	λ_{21} (Å)	A_{21} (sec ⁻¹)	$\Omega(1,2)$	λ_{31} (Å)	A_{31} (sec ⁻¹)	$\Omega(1,3)$	λ_{32} (Å)	A_{32} (sec ⁻¹)	$\Omega(3,2)$
O II	3,728.8	4.8×10^{-5}	1.43	2,470.4	0.060	0.428	7,319.4	0.115	1.70
	+3,726.0	+ 1.70×10^{-4}		+2,470.3	+0.0238		+7,330.7	+0.061	
							+7,318.6	+0.061	
							+7,329.9	+0.100	
O III	5,006.8 (N_1)	0.021	2.39	2,321.1	0.23	0.335	4,363.2	1.60	0.310
	+4,958.9 (N_2)	+0.0071							
N II	6,583.4	0.003	3.14	3,063.0	0.034	0.342	5,754.6	1.08	0.376
	+6,548.1	+0.00103							
Ne III	3,868.8	0.17	1.27	1,814.8	2.2	0.164	3,342.5	2.8	0.188
	+3,967.5	+0.052							
Ne IV	2,441.3	5.9×10^{-4}	1.04	1,608.8	1.33	0.427	4,714.3	0.40	1.42
	+2,438.6	+ 5.6×10^{-3}		+1,609.0	+0.53		+4,724.2	+0.44	
							+4,715.6	+0.11	
							+4,725.6	+0.39	
Ne V	3,425.9	0.38	1.38	1,575.2	4.2	0.218	2,972	2.60	0.185
	+3,345.8	+0.138							
S II	6,716.4	4.7×10^{-5}	3.07	4,068.6	0.34	1.28	10,320.6	0.21	6.22
	+6,730.8	+ 3.0×10^{-4}		+4,076.4	+0.134		+10,287.1	+0.17	
							+10,372.6	+0.087	
							+10,338.8	+0.20	
S III	9,532.1	0.064	4.97	3,721.7	0.85	1.07	6,312.1	2.54	0.961
	+9,069.4	+0.025		+3,796.7	+0.016				
Ar III	7,135.8	0.32	4.75	3,109.0	4.0	0.724	5,191.8	3.1	0.665
	+7,751.0	+0.083		+3,005.1	+0.043				
Ar IV	4,740.2	0.028	1.43	2,854.8	2.55	0.645	7,237.3	0.67	4.92
	+4,711.3	0.0022		+2,869.1	+0.97		+7,170.6	+0.91	
							+7,332.0	+0.122	
							+7,262.8	+0.68	
Ar V	7,005.7	0.51	1.19	2,691.4	6.8	0.141	4,625.5	3.78	0.945
	+6,435.1	+0.22		+2,784.4	+0.081				

¹ After GARSTANG (1968) and CZYZAK *et al.* (1968) by permission of the International Astronomical Union.

Spectroscopic Notation

Ionization State

I ---- neutral atom, e.g., H I \rightarrow H⁰

II --- singly ionized atom, e.g., H II \rightarrow H⁺

III – doubly ionized atom, e.g., O III \rightarrow O⁺⁺

..... and so on....e.g., Fe XXIII

Peculiar Spectra

e (emission lines), p (peculiar, affected by magnetic fields),
m (anomalous metal abundances), e.g., B5 Ve

Forbidden Lines

Allowed transitions (via an **electric dipole**) satisfying selection rules

1. Parity change
2. $\Delta L = 0, \pm 1, L = 0 \rightarrow 0$ forbidden
3. $\Delta J = 0, \pm 1, J = 0 \rightarrow 0$ forbidden
4. Only one electron with $\Delta \ell = \pm 1$
5. $\Delta S = 0$ (Spin not changed)

A forbidden transition is one that fails to fulfill at least one of the selection rules 1 to 4. It may arise from a **magnetic dipole** or an **electric quadrupole** transition.

Bowen (1936) Rev. Mod. Phys. 8, 55-81

The Origin of the Nebulium Spectrum.

IN the spectra of the gaseous nebulae several very strong lines are found which have not been duplicated in any terrestrial source. Many lines of evidence point to the fact that the lines are emitted by an element of low atomic weight. Since the spectra of the light elements, as excited in terrestrial sources, are well known, this leads to the conclusion that there must be some condition, presumably low density, which exists in the nebulae, that causes additional lines to be emitted.

since any jump between them involves a zero change in the azimuthal quantum number. In a five-electron system such as O_{II} , the normal configuration of 2 ($2s$) and 3 ($2p$) electrons forms 4S , 2D , and 2P terms. These are likewise metastable.

3726.16 O_{II} $^4S \rightarrow ^2D_2$

I. S. BOWEN.

Norman Bridge Laboratory of Physics,
California Institute of Technology,
Sept. 7.

REVIEWS OF MODERN PHYSICS

VOLUME 8

APRIL, 1936

NUMBER 2

Forbidden Lines

I. S. BOWEN, *California Institute of Technology*

TABLE OF CONTENTS

I. Introduction, (Ritz combination principle, empirical selection rules)	55	Five-electron systems, B I, C II, N III, O IV	67
II. Line Intensities (General considerations)	56	Six-electron systems, C I, N II, O III, F IV, Ne V	67
III. Transition Probabilities (Dipole, quadruple, etc. radiation terms)	57	(Variations in relative intensity of forbidden lines with density, high intensity of forbidden lines compared to permitted)	
IV. Quadrupole Radiation (and other "forbidden" types of radiation)	59	Seven-electron systems, N I, O II, F III, Ne IV	70
A. Selection rules, transition probabilities and line intensities	59	Eight-electron systems, O I, F II, Ne III, Na IV	72
B. Absorption coefficients and anomalous dispersion	60	(Auroral, nebular and transauroral lines)	
C. Zeeman effect	60	Nine-electron systems, F I, Ne II, Na III	73
V. Intensities of Forbidden Lines (as determined by physical conditions)	61	Ten-electron systems, Ne I, Na II, Mg III	73
A. Removal from the metastable state by collisions	61	Eleven-electron systems, Na I, Mg II, Al III	73
B. Removal from the metastable state by absorption	63	Twelve-electron systems, Mg I, Al II, Si III	73
VI. Physical Conditions and Mechanism of Excitation in the Nebulae	64	Thirteen-electron systems, Al I, Si II, P III, S IV	73
VII. Tables and Discussion of Forbidden Lines	65	Fourteen-electron systems, Si I, P II, S III, Cl IV, A V	74
One-electron systems, H I, He II	67	Fifteen-electron systems, P I, S II, Cl III, A IV, K V, Ca VI	75
Two-electron systems, He I, Li II	67	Sixteen-electron systems, S I, Cl II, A III, K IV, Ca V	76
Three-electron systems, Li I, Be II, B III, C IV	67	Seventeen-electron systems, Cl I, A II, K III	77
Four-electron systems, Be I, B II, C III, N IV, O V	67	Eighteen-electron systems, A I, K II, Ca III	78
		Elements of the first long period	78

- **Allowed (regular) Lines** (no bracket),
 $A \approx 10^{+8} \text{ s}^{-1}$, e.g., C IV
- **Semi-forbidden Lines** (a single bracket),
 $A \approx 10^{+2} \text{ s}^{-1}$, e.g., [OII]
- **Forbidden Lines** (a pair of square brackets),
 $A \approx 10^0 \text{ to } 10^{-4} \text{ s}^{-1}$, e.g., [O III], [N II]

Some examples,

Lyman α , $A_{21} \approx 6.25 \times 10^8 \text{ s}^{-1}$

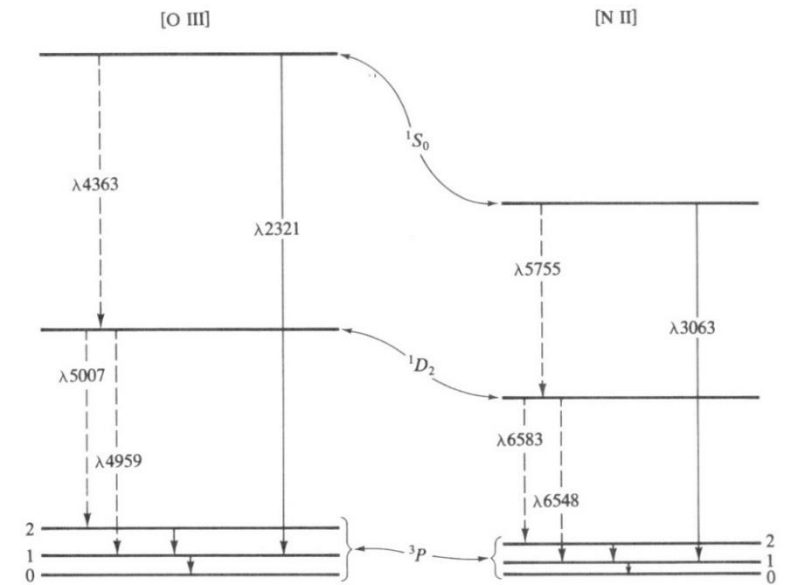
[O III] $A_{21} = 0.021 \text{ s}^{-1}$, $\lambda_{21} = 5007 \text{ \AA}$

$A_{21} = 0.0281 \text{ s}^{-1}$, $\lambda_{21} = 4959 \text{ \AA}$

$A_{32} = 1.60 \text{ s}^{-1}$, $\lambda_{32} = 4364 \text{ \AA}$

[S II] $A_{21} = 4.7 \times 10^{-5} \text{ s}^{-1}$, $\lambda_{21} = 6716 \text{ \AA}$

H I 21 cm hyperfine line $A_{21} \approx 2.88 \times 10^{-15} \text{ s}^{-1}$;
probability extremely low

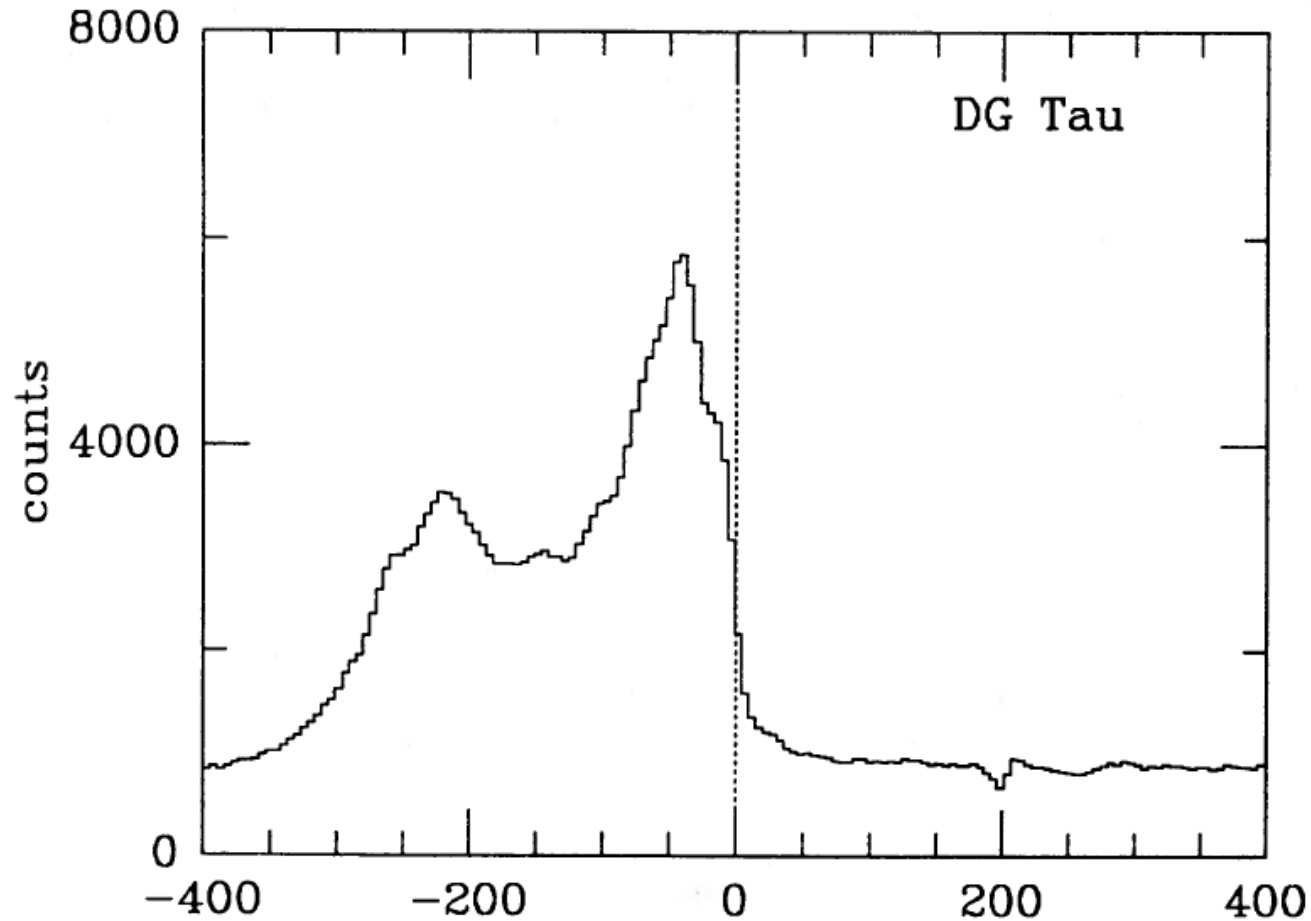


- Normally an atom stays in the excited state for 10^{-8} s.
- A forbidden transition occurs for excitation levels $<$ a few eV, and stays in the excited state for seconds or longer before returning to the ground state.
- In the lab $n \uparrow\uparrow$, both excitation and de-excitation take place frequently, so radiative transition (emitting a photon) is unlikely.
- In ISM, the electrons are not energetic enough to excite the atoms to normal levels (10 to 20 eV), but enough to excite to metastable levels. In hot, low-density environments, e.g., H II regions, PNe, solar corona, earth aurora
- Once (collisionally) excited \rightarrow emission
 \rightarrow photons escaped \rightarrow **efficient cooling**

Table 17.1 Main Emission Lines in Classical T Tauri Stars

Line	Transition	Wavelength (Å)	A_{ul} (s^{-1})
<i>Infrared</i>			
Br γ	$n = 7 \rightarrow 4$	21661	3.0×10^5
Pa β	$n = 5 \rightarrow 3$	12822	2.2×10^6
Ca II	$^2P_{1/2} \rightarrow ^2D_{3/2}$	8662	2.8×10^5
Ca II	$^2P_{3/2} \rightarrow ^2D_{5/2}$	8542	1.2×10^6
Ca II	$^2P_{3/2} \rightarrow ^2D_{3/2}$	8498	6.3×10^5
<i>Optical</i>			
[S II]	$^2D_{3/2} \rightarrow ^4S_{3/2}$	6731	8.8×10^{-4}
[S II]	$^2D_{5/2} \rightarrow ^4S_{3/2}$	6716	2.6×10^{-4}
H α	$n = 3 \rightarrow 2$	6563	1.0×10^8
[O I]	$^1D_2 \rightarrow ^3P_2$	6300	6.3×10^{-3}
Na I D ₁	$^2P_{1/2} \rightarrow ^2S_{1/2}$	5896	6.2×10^7
Na I D ₂	$^2P_{3/2} \rightarrow ^2S_{1/2}$	5890	6.2×10^7
He I	$^3D_3 \rightarrow ^3P_2$	5876	7.1×10^7
Fe II	$^6P_{3/2} \rightarrow ^6S_{5/2}$	4924	3.3×10^6
H β	$n = 4 \rightarrow 2$	4861	3.8×10^7
H γ	$n = 5 \rightarrow 2$	4340	1.6×10^7
Fe I	$^3F_3 \rightarrow ^3F_2$	4132	1.2×10^7
[S II]	$^2P_{1/2} \rightarrow ^4S_{3/2}$	4076	9.1×10^{-2}
Ca II H	$^2P_{1/2} \rightarrow ^2S_{1/2}$	3969	1.4×10^8
Ca II K	$^2P_{3/2} \rightarrow ^2S_{1/2}$	3934	1.5×10^8
<i>Ultraviolet</i>			
Mg II h	$^2P_{1/2} \rightarrow ^2S_{1/2}$	2803	2.6×10^8
Mg II k	$^2P_{3/2} \rightarrow ^2S_{1/2}$	2796	2.6×10^8
C IV	$^2P_{3/2} \rightarrow ^2S_{1/2}$	1548	2.7×10^8
Si IV	$^2P_{1/2} \rightarrow ^2S_{1/2}$	1403	7.6×10^8
O I	$^3S_1 \rightarrow ^3P_1$	1305	2.0×10^8
S I	$^3P_1 \rightarrow ^3P_2$	1296	4.9×10^8
Ly α	$2p \rightarrow 1s$	1216	6.3×10^8

The [O I]6300 profile of a T Tauri star; blueshifted wind



Inference: the redshifted emission is blocked by an optically thick dusty disk

Herbig-Haro objects: shocked excited nebulosity by young stars

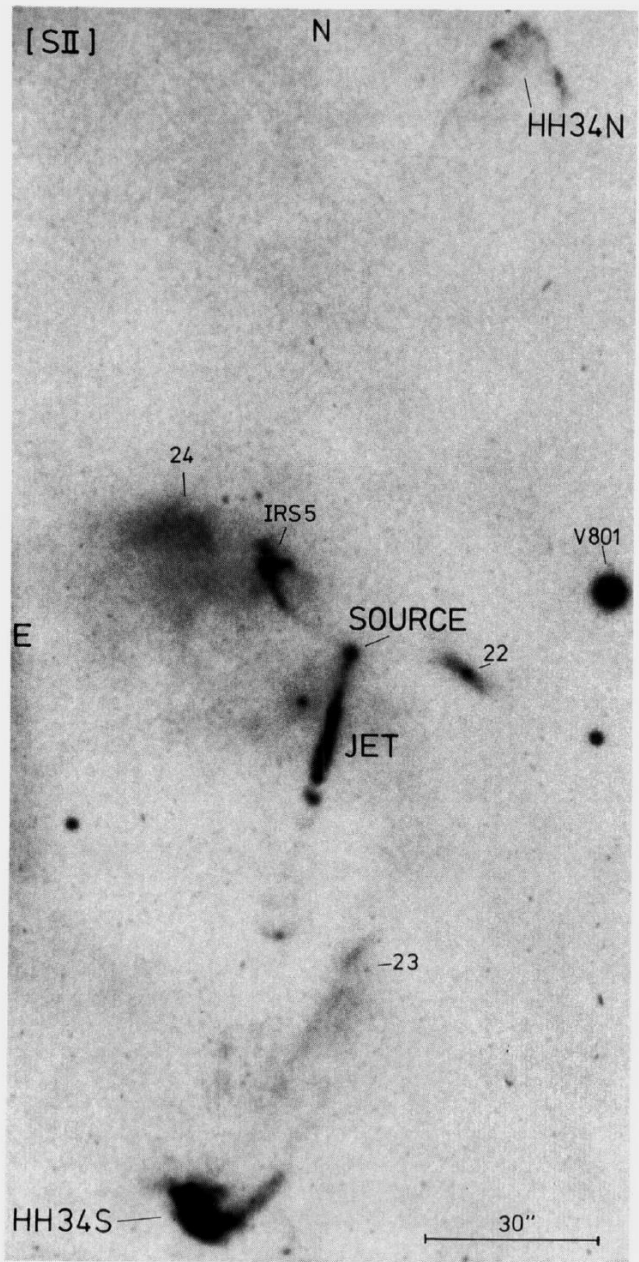
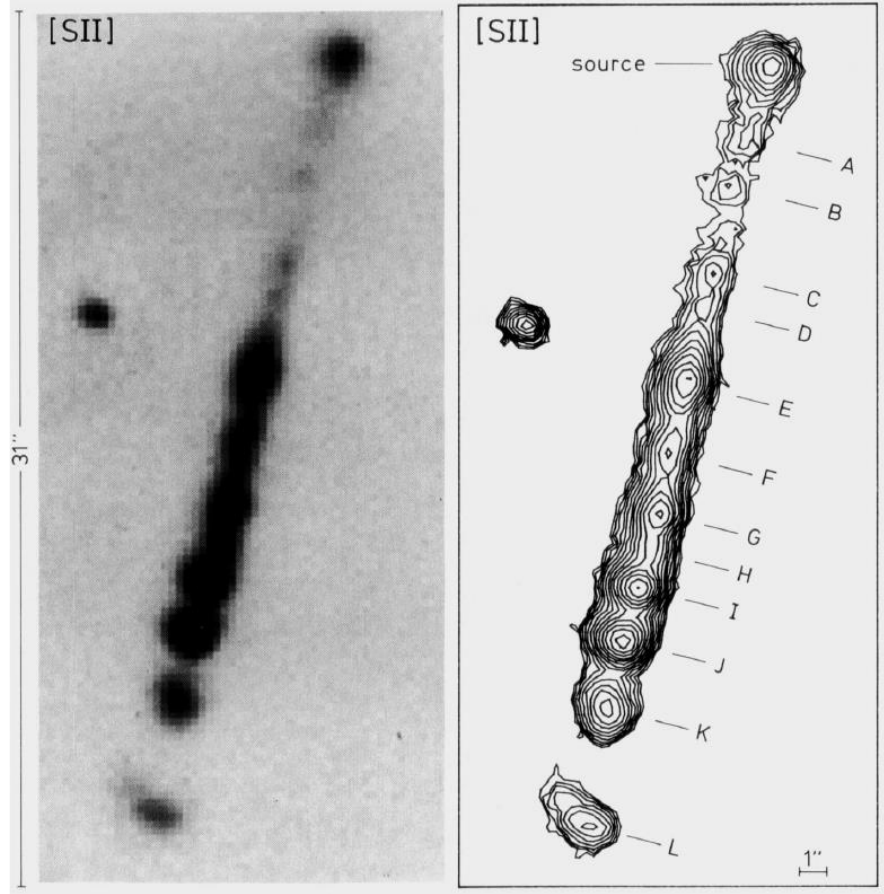


Fig. 1. A montage of two CCD-images of the HH 34-region taken through a [SII] 226716/6731 Å filter. The nebulous objects in this field are labeled according to Reipurth (1985b)



Bührke & Mundt (1988)

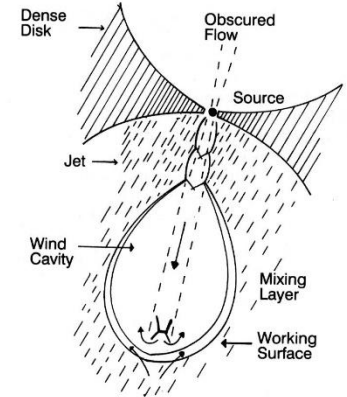


Figure 1. A diagram of a typical outflow from a young stellar object.

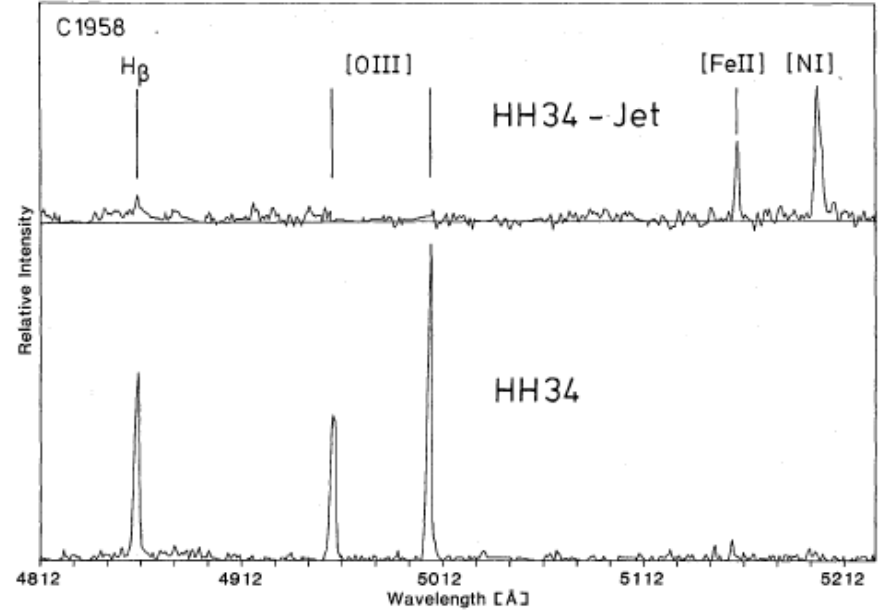


Fig. 5. Spectrum of the jet and HH 34S around the [OIII]-lines, demonstrating the different excitation conditions

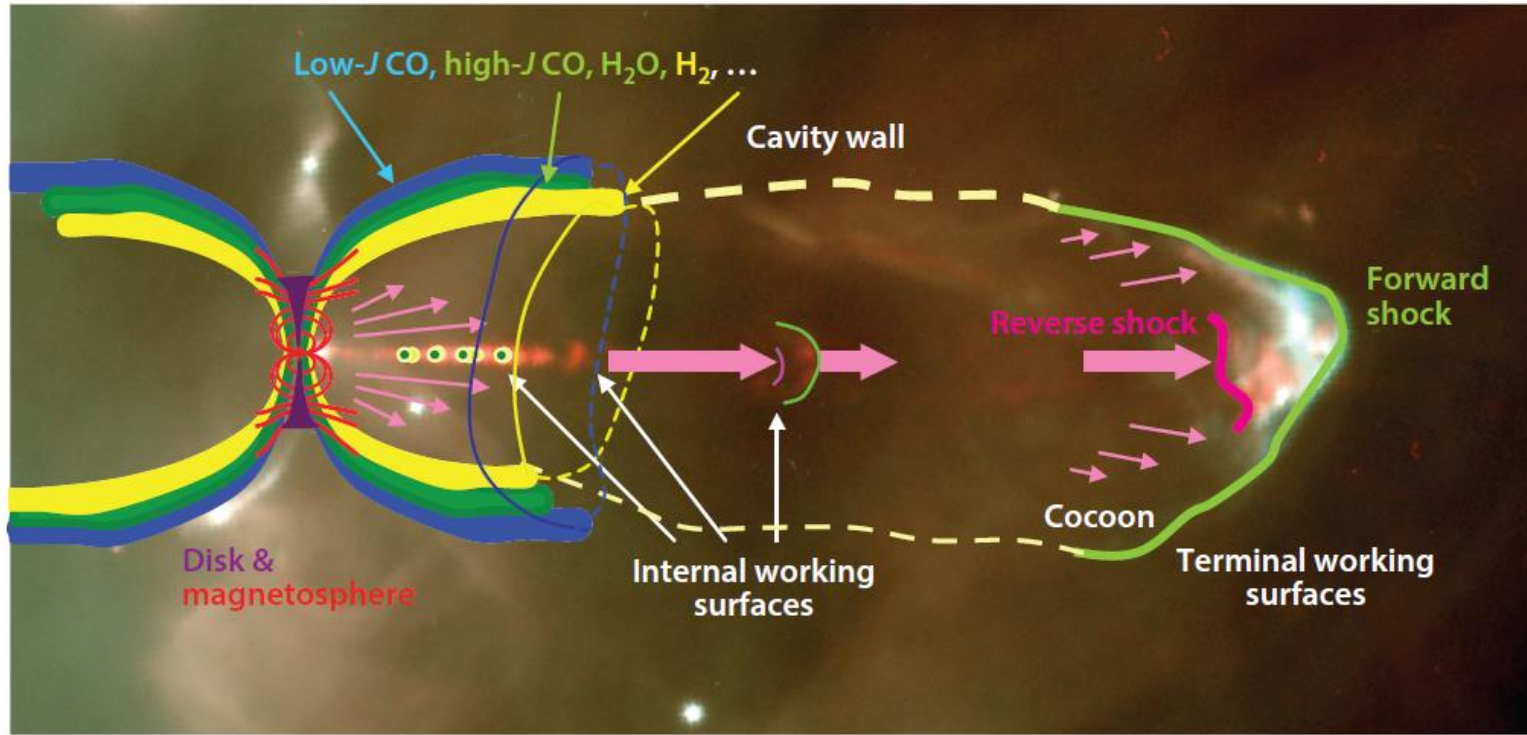
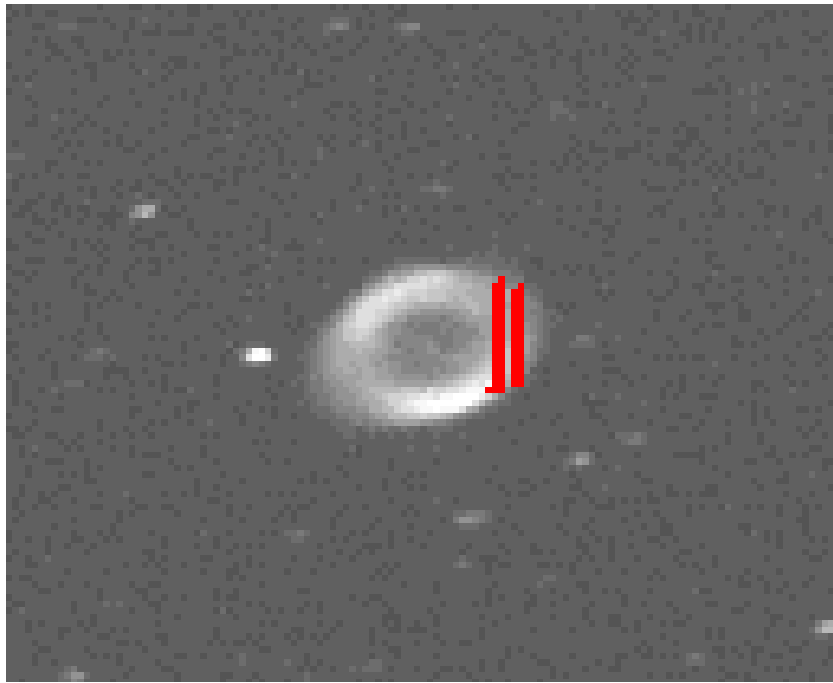


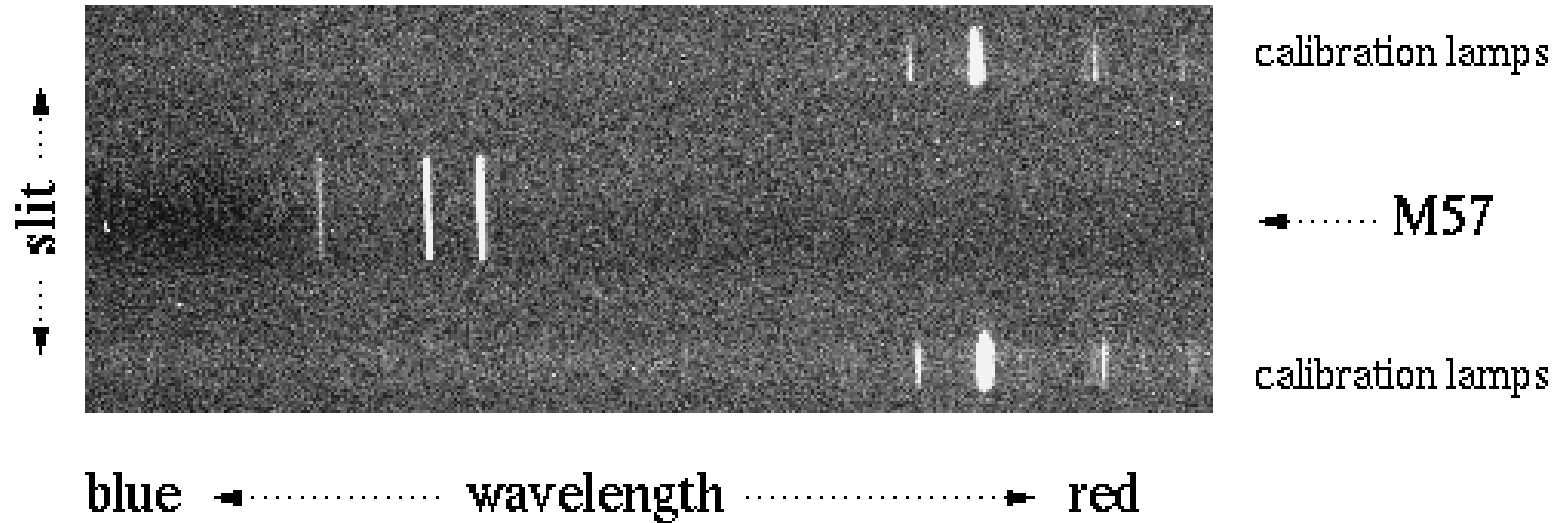
Figure 3

A cartoon showing the main components of a protostellar outflow lobe. The sizes of the disk (*purple*), the poloidal component of the disk and stellar magnetic fields (*red*), and the biconical molecular outflow are greatly exaggerated. The youngest outflows are compact, consisting of swept-up molecular shells powered by jets containing molecules. As they break out from their parent cores and grow to parsec scales, outflows become predominantly atomic or ionized and traced by Herbig-Haro (HH) objects. Molecules are usually confined to the outflow cavity walls near the source young stellar object but can also trace jets in the youngest flows. Thick, colored bands mark cavity shocks and UV-heated gas along the cavity walls, and spot-shocks mark supersonic velocity variations in the jet. Forward shocks are in bright green, and reverse shocks in magenta in both the terminal and internal working surfaces. Low- J CO is shown in blue, high- J CO in green, and shock-heated H_2 in yellow. The dashed, yellow line shows the predominantly atomic or ionized cavity wall. The underlying image shows a close-up of HH 34 and its driving jet in $H\alpha$ (*cyan*) and $[SII]$ (*red*).

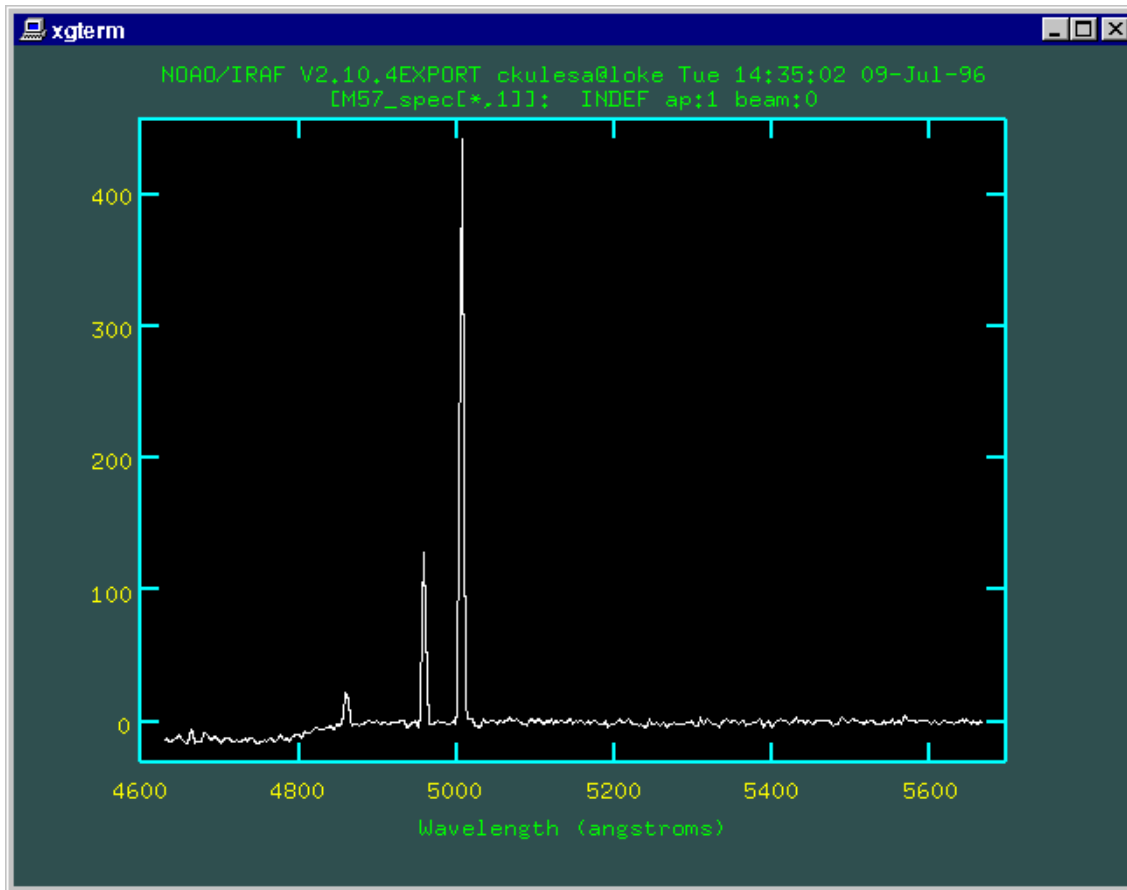


An example -----
Ring Nebula (M57),
a planetary nebula

Slit = 8' x 1"



http://loke.as.arizona.edu/~ckulesa/camp/camp_spectroscopy.html

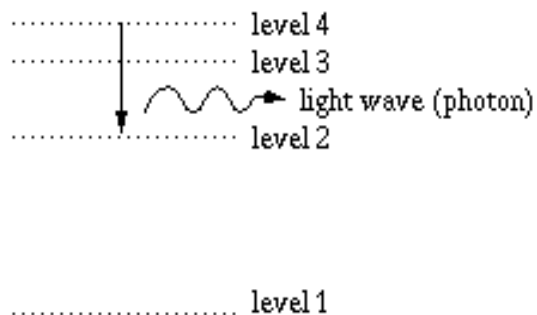


1-D spectrum shows little continuum, and a few emission lines

→ **A line spectrum**

4959Å and 5007Å doublet from twice-ionized oxygen, O⁺⁺, or OIII in spectroscopic notation

→ (oxygen) gas is ionized, with $T >$ a few thousand K and density $< 100/\text{cm}^3$



4861Å line from hydrogen

$$n = 4 \rightarrow 2$$

(called H_β line)

→ gas is highly excited

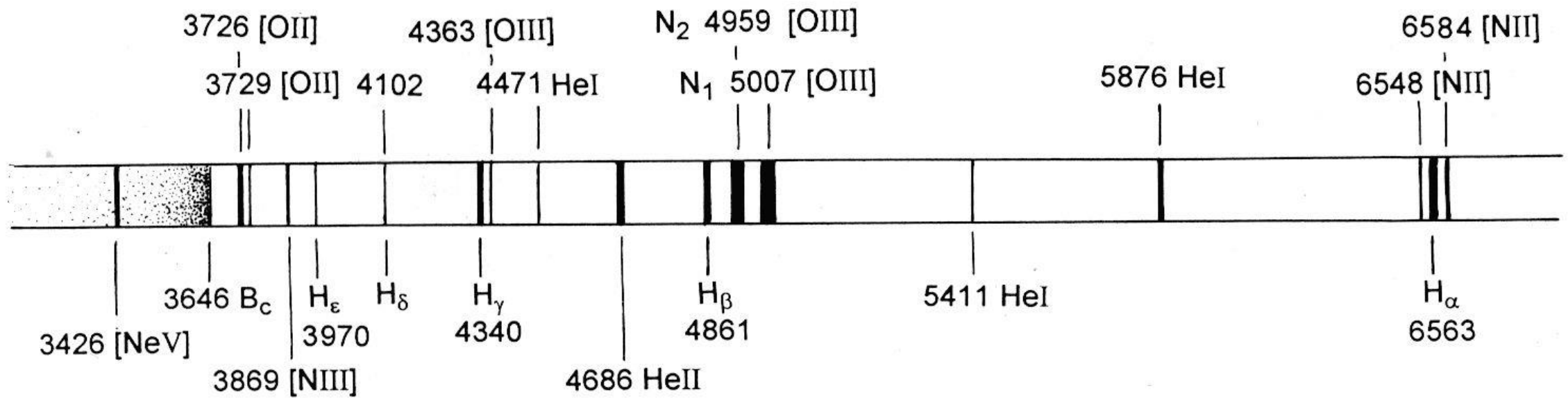


Fig. 1.1. General structure of the spectrum of a planetary nebula in the optical region, 3 300–7 000 Å. Only the most important emission lines, both permitted and forbidden, are shown. The shaded part from the left, beginning from $\lambda = 3\,646$ Å, is the Balmer continuum of hydrogen

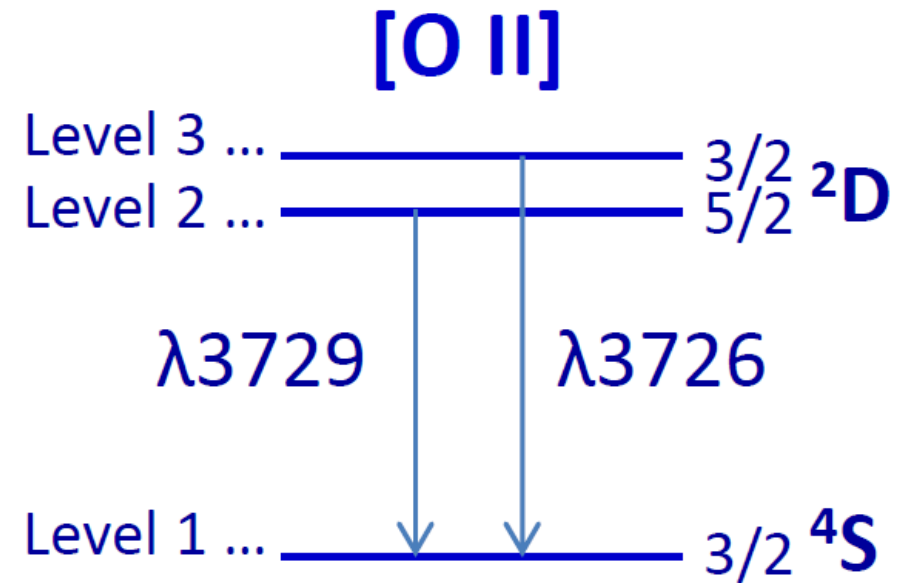
Excitation Theory --- Applications

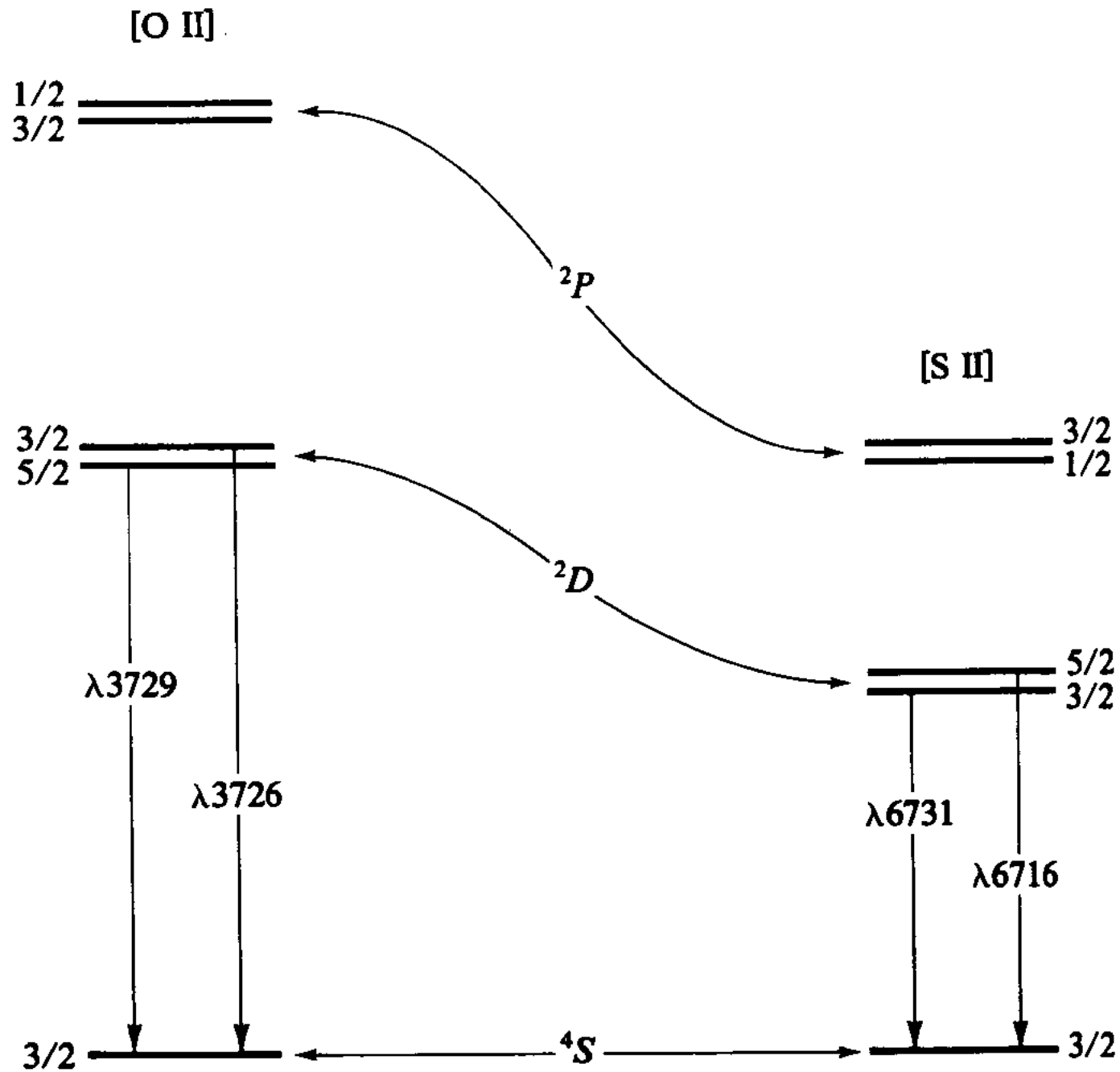
For [O II],

consider a 3-level system, with the two **upper** levels close together,

$$\frac{j_{\lambda 3729}}{j_{\lambda 3726}} = \frac{j_{21}}{j_{31}} = \frac{n_2 A_{21} h \nu_{21}}{n_3 A_{31} h \nu_{31}}$$

Note: $\Delta\lambda = 0.3 \text{ nm} \rightarrow$ need high-dispersion spectra





Osterbrock

$$\frac{j_{\lambda 3729}}{j_{\lambda 3726}} = \frac{j_{21}}{j_{31}} = \frac{n_2 A_{21} h \nu_{21}}{n_3 A_{31} h \nu_{31}}$$

✓ $n_e \rightarrow \infty$, collisional excitation and deexcitation

$$\frac{j_{21}}{j_{31}} = \frac{g_2 A_{21} \nu_{21}}{g_3 A_{31} \nu_{31}} e^{-E_{23}/kT} \approx \frac{g_2 A_{21}}{g_3 A_{31}} = \frac{6}{4} \frac{3.6 \times 10^{-5}}{1.8 \times 10^{-4}} = 0.3$$

Note: statistical weight $g = 2J + 1$

✓ $n_e \rightarrow 0$, every collisional excitation followed by emission

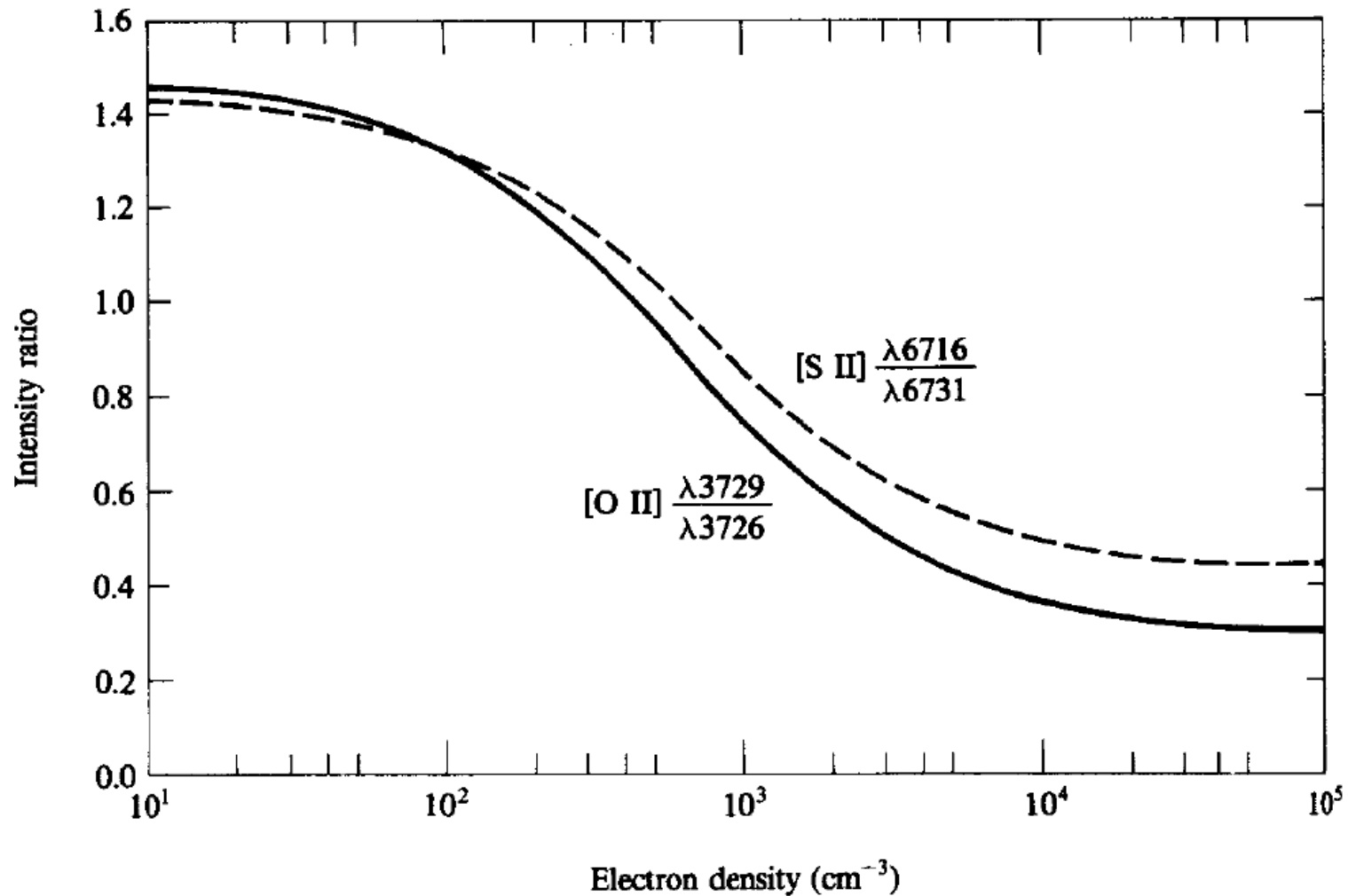
$$\frac{j_{21}}{j_{31}} = \frac{\gamma_{12}}{\gamma_{13}} = \frac{g_2}{g_3} e^{-E_{23}/kT} \approx \frac{g_2}{g_3} = \frac{6}{4} = 1.5$$

Because $\gamma_{21} \approx \gamma_{12}$, and $E_{23} \ll kT$

Transition of density limits occurs $n_{e,2} \approx 3 \times 10^3 \text{ cm}^{-3}$;

$n_{e,3} \approx 1.4 \times 10^4 \text{ cm}^{-3}$

So this kind of level configuration (upper close), the line ratio is sensitive to the electron number density.



Similar pairs of lines

[O II]

[S II]

[N I]

[Cl III]

[Ar IV]

[K V]

[Ne IV] λ2422, 2424

Some examples of density determinations for H II regions

TABLE 5.6

Electron densities in H II regions

Object	$\frac{I(\lambda 3729)}{I(\lambda 3726)}$	$N_e(\text{cm}^{-3})$
NGC 1976 A	0.50	3.0×10^3
NGC 1976 M	1.26	1.4×10^2
M 8 Hourglass	0.65	1.5×10^3
M 8 outer	1.26	1.5×10^2
NGC 281	1.37	7×10
NGC 7000	1.38	6×10

For planetary nebulae

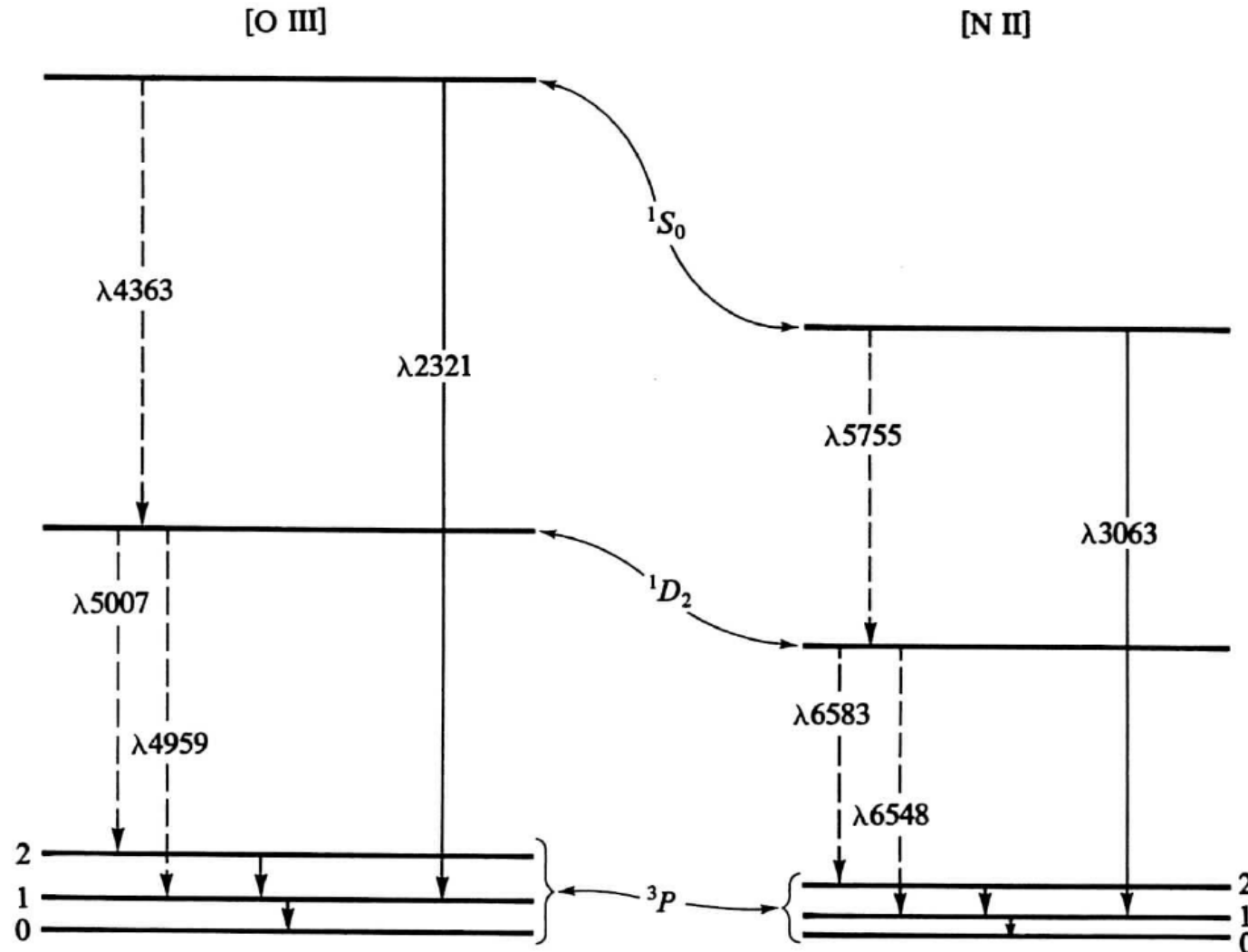
TABLE 5.7
Electron densities in planetary nebulae

Nebula	[O II]		[S II]	
	$\frac{\lambda 3729}{\lambda 3726}$	N_e^a (cm ⁻³)	$\frac{\lambda 6716}{\lambda 6731}$	N_e^a (cm ⁻³)
NGC 40	0.78	1.1×10^3	0.69	2.1×10^3
NGC 650/1	1.23	2.1×10^2	1.08	4.0×10^2
NGC 2392	0.78	1.1×10^3	0.88	9.1×10^2
NGC 2440	0.64	1.9×10^3	0.62	3.2×10^3
NGC 3242	0.62	2.2×10^3	0.64	2.8×10^3
NGC 3587	1.30	1.4×10^2	1.25	1.8×10^2
NGC 6210	0.47	5.8×10^3	0.66	2.5×10^3
NGC 6543	0.44	7.9×10^3	0.54	5.9×10^3
NGC 6572	0.38	2.1×10^4	0.51	8.9×10^3
NGC 6720	1.04	4.7×10^2	1.14	3.2×10^2
NGC 6803	0.57	2.8×10^3	—	—
NGC 6853	1.16	2.9×10^2	—	—
NGC 7009	0.50	4.6×10^3	0.61	3.3×10^3
NGC 7027	0.48	5.2×10^3	0.59	4.0×10^3
NGC 7293	1.32	1.3×10^2	1.28	1.6×10^2
NGC 7662	0.56	3.0×10^3	0.64	2.8×10^3
IC 418	0.37	3.2×10^5	0.49	9.5×10^3
IC 2149	0.56	3.0×10^3	0.57	4.6×10^3
IC 4593	0.63	2.0×10^3	—	—
IC 4997	0.34	1.0×10^6	0.45	1.0×10^5

Osterbrock

^a N_e given for assumed $T = 10^4$ ° K; for any other T divide listed value by $(T/10^4)^{1/2}$.

Now consider a different level configuration with [O III] or [N II], for which the two **lower** levels are close together.



Osterbrock

So

$$\frac{j_{4959} + j_{5007}}{j_{4363}} = \frac{\Omega_{(3P,1D)}}{\Omega_{(3P,1S)}} \left[\frac{A_{(1S,1D)} + A_{(1S,3P)}}{A_{(1S,1D)}} \right] \frac{\bar{\nu}_{(3P,1D)}}{\nu_{4363}} \exp(\Delta E/kT)$$

$$\approx \frac{7.73 \exp[(3.29 \times 10^4)/T]}{1 + 4.5 \times 10^{-4}(N_e/T^{1/2})} = \frac{7.15}{1 + 0.0028 x} 10^{14300/T_e}$$

where

$$\bar{\nu} = \frac{A_{(1D,3P_2)} \nu_{5007} + A_{(1D,3P_1)} \nu_{4959}}{A_{(1D,3P_2)} + A_{(1D,3P_1)}} \quad x = \frac{0.01 n_e}{\sqrt{T_e}}$$

and ΔE is the energy difference between 1D and 1S .

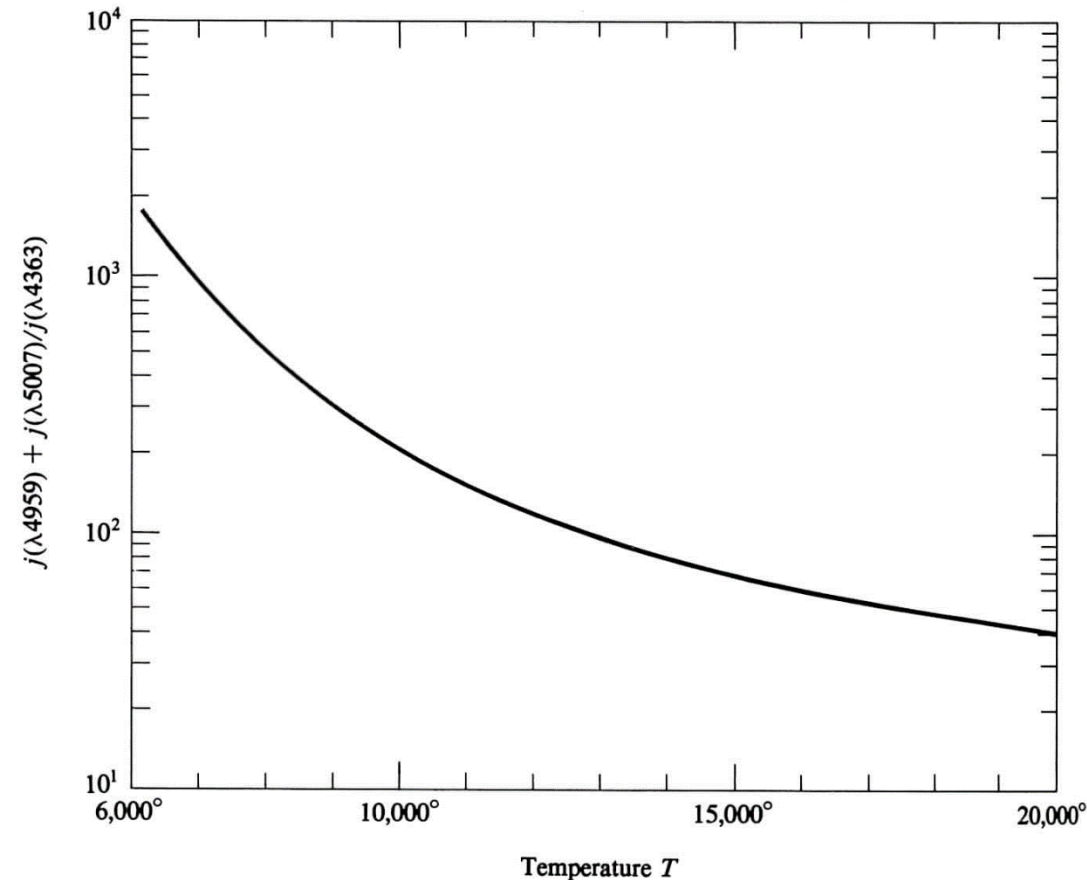
This holds up to $n_e \approx 10^5 \text{ cm}^{-3}$.

At higher densities, collisional de-excitation begins to play a role.

Similarly, for [N II],

$$\frac{j_{6548} + j_{6583}}{j_{5755}} \approx \frac{6.91 \exp[(2.50 \times 10^4)/T]}{1 + 2.5 \times 10^{-3}(N_e/T^{1/2})} = \frac{8.5}{1 + 0.29 x} 10^{10800/T_e}$$

So with this kind of level configuration (lower close; [O III] or [N II]), the line ratio is sensitive to temperature.



Problems:

1. I_{4959} and I_{5007} are strong but I_{4363} is weak
2. I_{4363} is close to Hg I $\lambda 4358$ (sky!)

Osterbrock

Some examples of temperature determinations ...

TABLE 5.1
Temperature determinations in H II regions

Nebula	[N II]			[O III]	
	$\frac{I(\lambda 6548) + I(\lambda 6583)}{I(\lambda 5755)}$	$T(^{\circ} \text{K})$	$N_e/T^{1/2}$	$\frac{I(\lambda 4959) + I(\lambda 5007)}{I(\lambda 4363)}$	$T(^{\circ} \text{K})$
NGC 1976 2b	81	10,000	51	338	8,700
NGC 1976 1a	102	9,100	68	371	8,500
NGC 1976 5b	111	8,900	21	310	8,900
NGC 1976 5a	189	7,500	12	263	9,300
M 8 I	162	7,900	(10)	445	8,100
M 17 I	257	6,900	(10)	330	8,700
NGC 2467 1a	46	13,000	(1)	129	11,600
NGC 2467 1b	53	12,200	(1)	137	11,400
NGC 2359 av	—	—	(1)	90	13,200

TABLE 5.2
*Temperature determinations
 for planetary nebulae*

Nebula	$T[\text{N II}]$ (° K)	$T[\text{O III}]$ (° K)
NGC 650	9,500	10,700
NGC 4342	10,100	11,300
NGC 6210	10,700	9,700
NGC 6543	9,000	8,100
NGC 6572	—	10,300
NGC 6720	10,600	11,100
NGC 6853	10,000	11,000
NGC 7027	—	12,400
NGC 7293	9,300	11,000
NGC 7662	10,600	12,800
IC 418	—	9,700
IC 5217	—	11,600
BB 1	10,500	12,900
Haro 4-1	—	12,000
K 648	—	13,100

Typically $T \sim 10,000$ K

ELECTRON TEMPERATURES IN PLANETARY NEBULAE

JAMES B. KALER

Astronomy Department, University of Illinois

Received 1985 November 4; accepted 1986 February 12

ABSTRACT

Electron temperatures for 107 planetary nebulae are calculated with the most recent atomic parameters from [O III] or [N II] line intensities or both taken from a variety of sources. The two temperatures exhibit quite different variations with respect to nebular ionization level, or excitation. Within somewhat broad limits, $T_e[\text{O III}]$ can be taken as constant at 10,200 K for nebulae without He II $\lambda 4686$; with the onset of that line, this temperature quickly climbs according to $T_e[\text{O III}] = 9700 \text{ K} + 58I(\lambda 4686)$, where the line intensity is scaled as usual to $I(\text{H}\beta) = 100$. $T_e[\text{N II}]$ behaves oppositely. With $\lambda 4686$ present, there is little discernable trend with excitation around a median value of 10,300 K; as the excitation drops and $\lambda 4686$ disappears, this temperature appears first to increase, and then to decrease to values well below 8000 K: for $\log T_*$ (central star temperature) < 4.7 , $T_e[\text{N II}] = 14,670 \log T_* - 57,330$. The dispersion in T_e for a specific excitation correlates negatively with O/H as expected.

Combination of the [O III] and [N II] data sets shows that the mean ratio of $T_e[\text{N II}]/T_e[\text{O III}] = \bar{r}$ varies smoothly and strongly also as a function of overall nebular excitation. As excitation increases from $T_* \approx 25,000 \text{ K}$ to $\sim 50,000 \text{ K}$, \bar{r} increases from ~ 0.7 to ~ 1.1 . It then decreases through the onset of He^{+2} , dropping to 0.7 again for the highest levels of ionization, that is, the nebular temperature gradient as inferred from O^{+2} and N^+ is usually negative with respect to distance from the central star but reverses to positive for nebulae in the midrange of excitation for $T_* \approx 50,000 \text{ K}$.

Comparison of [O III] temperatures among major reference sources shows clear systematic differences. The observations by French and by Torres-Peimbert and Peimbert yield the highest values, roughly 1000 K higher than those obtained from Aller and Czyzak and from Barker. No such trends are seen for $T_e[\text{N II}]$, possibly because the scatter in the data is considerably larger.

Read the paper by Donald Menzel

1937ApJ...85..330M

PHYSICAL PROCESSES IN GASEOUS NEBULAE

I. ABSORPTION AND EMISSION OF RADIATION

DONALD H. MENZEL

ABSTRACT

In this paper, the first of a series dealing with the physical state of gaseous nebulae, various fundamental formulae are derived. The total emission and absorption of radiation by atomic hydrogen are evaluated, together with the number of transitions to and from any quantum level, discrete or continuous. The equations are thrown into simple homogeneous form. The general equations that determine the statistical equilibrium of the assembly and the partition of atoms into various atomic states are developed. Solution of these equations is deferred until a later paper.